Summer 2004

A Search for Infrared Emission from Circumpulsar Disks and Compact Objects

L. Blecha and M. Jura

Dept. of Physics and Astronomy, University of California, Los Angeles

ABSTRACT

We propose to measure infrared fluxes from eleven pulsars using the IRAC and MIPS instruments on the Spitzer Space Telescope. Our goals are to detect thermal emission from circumpulsar dust disks and determine whether such disks are common. In addition, we will observe the cataclysmic variable AE Aqr, which has been detected at mid-IR wavelengths in excess of a Rayleigh-Jeans tail from the secondary star, and also the microquasar SS 433, which has not yet been observed with Spitzer.

1. INTRODUCTION

The discovery of planets around pulsar B1257+12 (Wolszczan & Frail 1992) created great interest in the questions of how planets form around pulsars and whether other pulsars have planetary systems. As planets are understood to form from circumstellar disks of dust and other material, it is logical to examine how protoplanetary disks might form around pulsars. The planets around B1257+12 orbit between 0.19 and 0.49 AU - too close to have existed during the star's red giant phase (Drilling & Landolt 1999). The supernova explosion would also disrupt any existing planetary or protoplanetary systems; thus, a circumpulsar disk must form after these evolutionary stages. One possibility is a fallback disk formed from ejected material that falls back onto the neutron star after the supernova. Such a disk would absorb some energy from the pulsar's 'spin-down' luminosity - radiation which causes rotational energy loss and slows the rapidly spinning pulsar over time - and re-radiate at cooler, mostly infrared wavelengths that theoretically could be observed from earth.

Currently, there is little concrete evidence for circumpulsar disks, but indirect evidence from previous observations leaves open the possibility of their existence. Several observations have been conducted, but have succeeded only in placing upper limits on disk masses. Foster

and Fischer (1996) created a model for the structure of the hypothetical disks. They conducted observations at 10 microns of five millisecond pulsars (MSP's) using NASA's Infrared Telescope Facility (IRTF), finding upper flux limits of 30-40 mJy. A more recent Infrared Space Observatory (ISO) observation (Joseph, Lazio, and Fischer 2004) constrained upper emission limits to 100mJy for the MSP's observed. Both upper limits are about factor of 10 to 10^3 greater than our predicted fluxes. Another search for IR excess around nine radio pulsars (Loehmer et al. 2004) suggested that if these pulsars have circumstellar disks, the disks are not massive enough to support planet formation. All of these studies concluded that more sensitive instruments, such as those on the Spitzer Space Telescope, are needed to search for disks that may be fainter than the limits of previous observations.

Cataclysmic variables (CV's) have also recently attracted attention from infrared observers. These objects are mass-transferring binary systems consisting of a white dwarf primary star and a main-sequence secondary star. In the evolution of a CV from a detached, long period binary system to a close, interacting binary, a significant amount of orbital angular momentum is lost. Magnetic braking was thought to be the primary mechanism for this process, but it has recently been discovered that the contribution of magnetic braking is significantly lower than had previously been calculated (Andronov, Pinsonneault & Sills 2003). Several theories have been suggested to explain the discrepancy between theory and observation, including the possibility of a circumbinary disk (CB) of cool material which extracts angular momentum through torque exerted on the CV. The CB material could originate from several sources, including accretion disk wind or synchrotron emission from clouds of gas expelled by the white dwarf (Dubus et al. 2003). The disks could theoretically be observed as excess infrared emission from the source, especially at mid-IR wavelengths where the secondary star does not dominate the spectral distribution. Near-IR observations of CV's have found some instances of excess IR emission, but none have conclusively determined the emission to be from a CB disk. Until recently, mid- and far-IR searches for CB disks had not been conducted. In 2003, observations with Keck detected mid-IR fluxes from SS Cyg and AE Aqr well above the secondary star contribution (Dubus et al.). The detection of AE Aqr is well explained by synchrotron emission from relativistic matter ejected by the rapidly spinning white dwarf. This hypothesis cannot be proven, however, without more sensitive observations using Spitzer. The emission from SS Cyg is less well-understood, but as a Spitzer program is currently scheduled for this source, we will focus our observation on AE Aqr.

SS 433, the first discovered microquasar, is a well-studied but still mysterious object. Many questions remain concerning the nature of the accreting black hole, the formation and composition of relativistic jets emitted by the black hole, and the evolution of microquasars in general. Because SS 433 is a bright source, it has been observed across the electromagnetic

spectrum since its discovery. Early IR observations demonstrated that the microquasar's periodic variation could be seen at infrared wavelengths (Margon 1984). An IRAS observation of SS 433 detected 'knots' of far-infrared emission, but was inconclusive as to whether the knots were associated with the relativistic jets, or with another source entirely (Band 1987). A later ISOPHOT observation used mid-IR spectra to confirm that the companion star to the compact object is a Wolf-Rayet-like star - the second such system discovered after Cygnus X-3 (Fuchs, Koch-Miramond, & Abraham 2002). Spitzer provides an opportunity to study the infrared emission from this intriguing source with unparalleled sensitivity; thus, we have included SS 433 in our observing program.

2. PULSAR DISK MODELS

2.1. Model A

To design IR observations of pulsars, we created a schematic model of the disk structure. Modeling the disks is problematic because little is known about their structure or composition. Thus, we designed a simple model using only information about the pulsar's distance from earth and its spin-down luminosity, along with a few basic assumptions. The total spin-down luminosity is $L_{SD} = 4\pi^2 I \dot{P} / P^3$, where the moment of inertia I is assumed to be $10^{45}\, g\, cm^2$ (Foster & Fischer 1996). The energy absorbed by the dust grains is some fraction of the total L_{SD}, which gives the total flux observed at earth

$$F_{tot} = \frac{f\, L_{SD}}{4\pi d^2}. \tag{1}$$

We assume the fraction absorbed f is about 1%, as estimated by Foster and Fischer (1996). It is also assumed that the dust grains radiate as black bodies. Then, the flux as a function of frequency is simply Planck's function with some arbitrary constant F_o that depends on factors of geometry and composition:

$$F_\nu = F_o \frac{\nu^3}{e^{h\nu/kT} - 1} \tag{2}$$

Integrating to get the total flux and combining this with (2) eliminates the arbitrary constant. Equating the result with (1) yields an expression for F_ν that does not depend on knowledge of the nature of the disk:

$$F_\nu = 15 F_{tot} \left(\frac{h}{\pi kT}\right)^4 \frac{\nu^3}{e^{h\nu/kT} - 1} \tag{3}$$

where F_{tot} is defined in (1).

To see the relationship between disk radius and temperature within this model, an annulus of dust at a single temperature was assumed. Using geometry and the Stefen-Boltzmann law to derive the relationship

$$R_{ring} = \left(\frac{f\, L_{SD}}{16\pi\sigma T_{ring}^4} \right)^{1/2} \tag{4}$$

we found that a temperature of 100K corresponds to 1 AU. Assuming 100K as a reasonable mean for dust temperatures, we adopted the 1 AU annulus model.

2.2. Model B

Given the considerable unknowns involved, we also considered an alternate model for comparison. Jura (2003) created a dust disk model to explain infrared excess observed around the white dwarf G29-38. This model was then used by Jura and Taylor (2003) to design IR observations of five pulsars. Assuming a flat, optically thin disk, it absorbs some energy $E = L_{SD} \cos\theta \,/\, 4\pi d^2$ from the star, where theta is the average incident angle of radiation. The disk temperature is then given by:

$$T_{disk} \approx \left(\frac{L_{SD} R_*}{3\pi^2 \sigma d^3} \right)^{1/4}. \tag{5}$$

R_* is assumed to be 10 km, an average value for pulsars. The dependence of temperature on radius allows the disk radius to be represented as $x = h\nu \,/\, kT$. A lower limit on disk radius is found by setting 1000K as the maximum temperature (the approximate temperature of sublimation for dust grains); the upper limit on radius is effectively infinite as fluxes fall off quickly at large radii. 0 degrees is the disk's assumed angle of incidence, and the frequency-dependent flux from the disk is:

$$F_\nu = \cos i \, \frac{16\pi h \nu^{1/3}}{3c^2 d^2} \left(\frac{L_{SD} R_* k^4}{6\pi^2 \sigma h^4} \right)^{2/3} \int_{x_{in}}^{x_{out}} \frac{x^{5/3}}{e^x - 1} dx \tag{6}$$

2.3. Limitations of the Models

Both models are simplified idealizations, but suitable for predicting a range of fluxes from which to design observations. Neither model is very reliable when pushed to extremes, but observing behavior of both models in this situation provides useful insight as to their limitations. Fig. 1 plots the spectral distribution of Pulsar J0437-4715 as calculated by both

models. At 8 μm, the models agree quite well, but Model A varies over a much wider range of fluxes than does Model B.

The distribution for Pulsar J2229+6114 (Fig. 2) is quite different - this star is at a much further distance of 12 kpc, as opposed to 140 pc, and has a factor of 10^3 greater luminosity. Model A has a much stronger dependence on luminosity, while Model B depends inversely on the pulsar distance. This causes the very high and low fluxes, respectively, seen in Fig. 2. In this case, the second model predicts fluxes below Spitzer sensitivites, and the first model must be used. For stars with even higher luminosities, however, the first model predicts fluxes too high to be plausible.

3. TARGET SOURCES

Pulsars were chosen based on information from the Australia Telescope National Facility (ATNF) Pulsar Database. We chose 11 pulsars that had high predicted fluxes and low background and source confusion (Table 1). Flux estimates from nearby infrared sources were obtained by Rayleigh-Jeans extrapolation of 2MASS data. The Spitzer Planning Observations Tool (SPOT) provided estimates of zodiacal light and other background radiation.

We also chose two compact objects to observe with Spitzer. AE Aqr was chosen as a CV source, and microquasar SS 433 was chosen as an additional source of interest.

4. OBSERVATIONS

4.1. Pulsars

We plan to observe these sources with the Infrared Array Camera (IRAC) and the Multiband Imaging Photometer for Spitzer (MIPS). The plots in Fig. 3 show the spectral distribution predicted by each model for both IRAC bands (3.6, 4.5, 5.8, & 8.0 μm) and for MIPS (24 and 70 μm). Using the most conservative flux estimates which fell within the instruments' capabilities, along with telescope sensitivity tables, we determined the necessary observation time for at least a 10-σ detection. We used SPOT to design the Astronomical Observing Request (AOR) for each pulsar based on this time estimate. For IRAC observations, a small dither pattern was implemented to correct for cosmic rays, bad pixels, etc. The MIPS Photometry mode automatically dithers around the source. Total observing times, including overhead as calculated by SPOT, are detailed in Tables 2 & 3.

4.2. AE Aqr

We will also observe AE Aqr at both IRAC and MIPS wavelengths. Using the mid-IR fluxes measured by Dubus et al. (2003), and following the conservative assumption that all of the near-IR flux is from the secondary star, we calculate mid-IR excesses of 10-20 mJy. We assumed these values for the IRAC bands, and used a Rayleigh-Jeans extrapolation of this excess radiation at the longer MIPS wavelengths. We used our predictions, with sensitivity tables and the SPOT features, to calculate an appropriate observing time estimate. Because AE Aqr is a very bright source, it would saturate the IRAC instrument in its full-array mode. Thus, we use the subarray mode to achieve a composite of $64 \times 0.1s$ and repeat once. A small dither pattern is also used.

For the MIPS AOR, only a short observing time is needed at 24 μm, so we use a frame of $1 \times 3s$. The predicted flux at 70 μm is much lower, so $10 \times 10s$ frames are used. The total observing time for AE Aqr, including overhead, is 0.69h.

4.3. SS433

To estimate fluxes for SS 433, near-IR flux data was obtained from 2MASS and extrapolated to longer wavelengths. This microquasar, like AE Aqr, is a very bright source, so the same subarray mode and dither pattern are necessary. We use slightly longer observation ($3 \times 3s$) at 24 μm than that for AE Aqr due to the lower predicted flux. The same frame time and repeat is used for 70 μm, and the total observation time for SS 433 is .72h.

5. SUMMARY

We have designed a Spitzer program to observe a sample of pulsars with the IRAC and MIPS instruments; our objective is to detect thermal emission from circumstellar disks around these objects, if they exist. To estimate appropriate observation times, we compared two dust models. Because Spitzer's instruments allow for much more sensitive pulsar observations than those previously conducted, a non-detection would enable us to place strong upper limits on disk masses. A detection of circumpulsar dust would answer many questions about the behavior of fallback disks, disk structure and composition, and the ability of such disks to form planetary systems like that of B1257+12.

We furthermore plan to conduct IRAC and MIPS observations of two compact object sources: AE Aqr and SS 433, with the goal of gaining insight into the evolution of these

unusual supernova remnants. The observation will use Guaranteed Time Observer (GTO) time, and our total requested observing time is 4.9h.

REFERENCES

Andronov, N., Pinsonneault, M., Sills, A. 2003, ApJ, 582, 358

Band, D. 1987, PASP, 99, 1269

Drilling, J. S., Landolt, A. U. 1999, Allen's Astrophysical Quantities, 381

Dubus, G., Campbell, R., Kern, B., Tamm, R. E., Spruit, H. C. 2003, SF2A-2003: Semaine de l'Astrophysique Francaise, 589

Foster, R. S., Fischer, J. 1996, ApJ, 460, 902-5

Fuchs, Y., Koch-Miramond, L., Abraham, P. 2002, SF2A-2002: Semaine de l'Astrophysique Francaise, 317

Joseph, T., Lazio, W., Fischer, J. 2004, AJ, 128, 842-5

Jura, M., 2003, ApJ, 584, L91-4

Jura, M., Taylor, J., 2003, Spitzer proposal

Loehmer, O., Wolszczan, A., Wielebinski, R. 2004, preprint(astro-ph/0406602)

Margon, B. 1984, ARA&A, 22, 519

Rosalba, P., Hernquist, L., Narayan, R. 2000, ApJ, 541, 344

Wolszczan, A., Frail, D. A. 1992, Nature, 355, 145-7

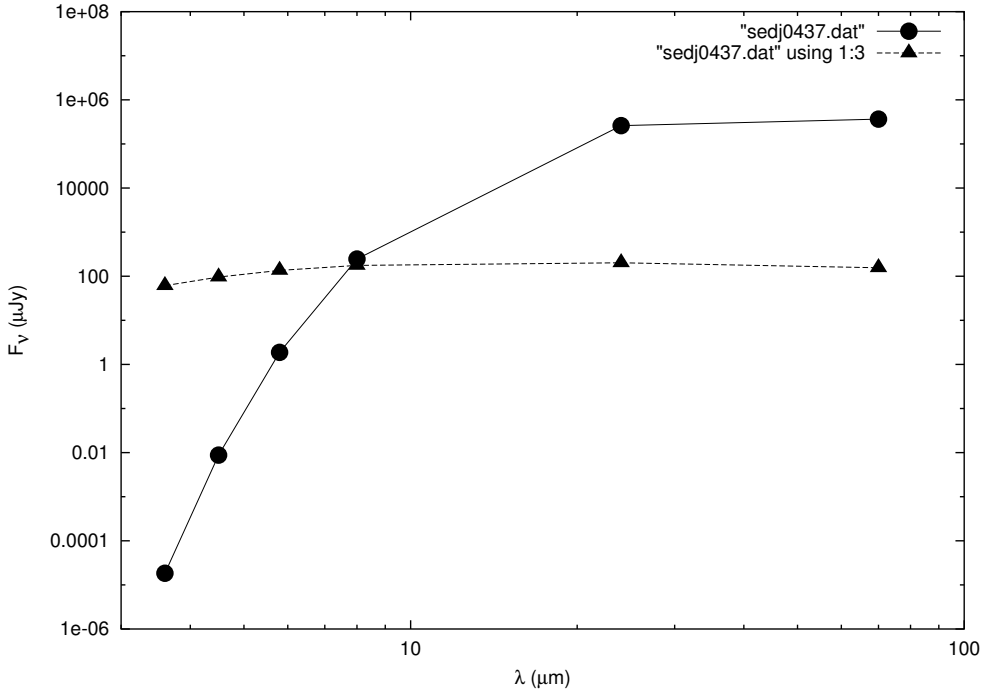

Fig. 1.— Predicted spectral distribution for J0437-4715 ($d = 140pc$, $L_{SD} = 1.2 \times 10^{34} erg/s$). The circles and triangles denote models A and B, respectively.

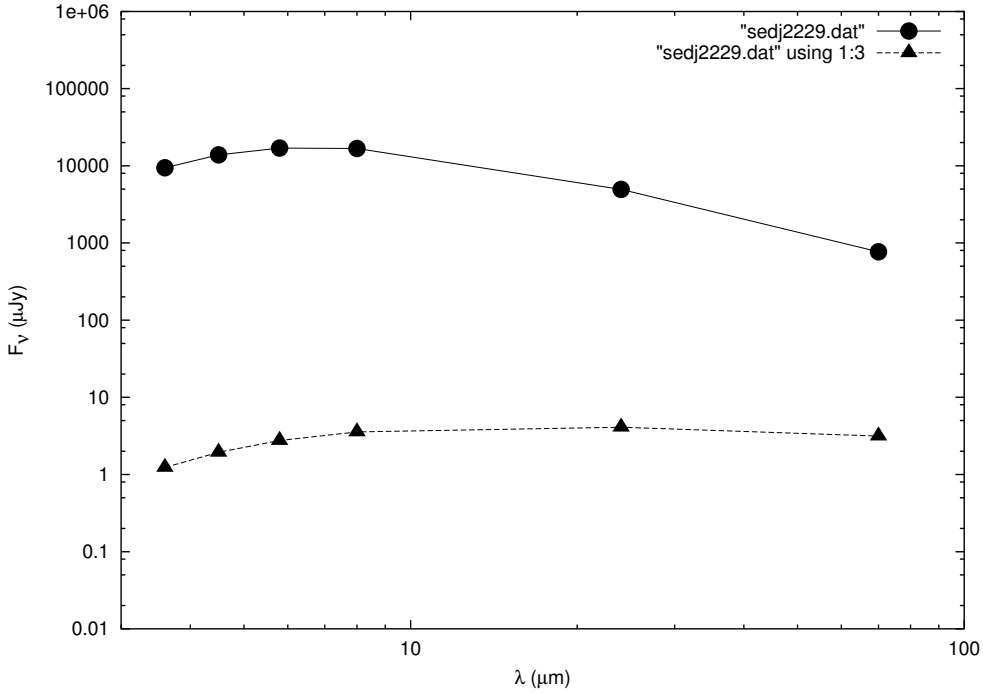

Fig. 2.— Predicted spectral distribution for J2229+6114 ($d = 12.03kpc$, $L_{SD} = 2.2 \times 10^{37} erg/s$). The circles and triangles denote models A and B, respectively.

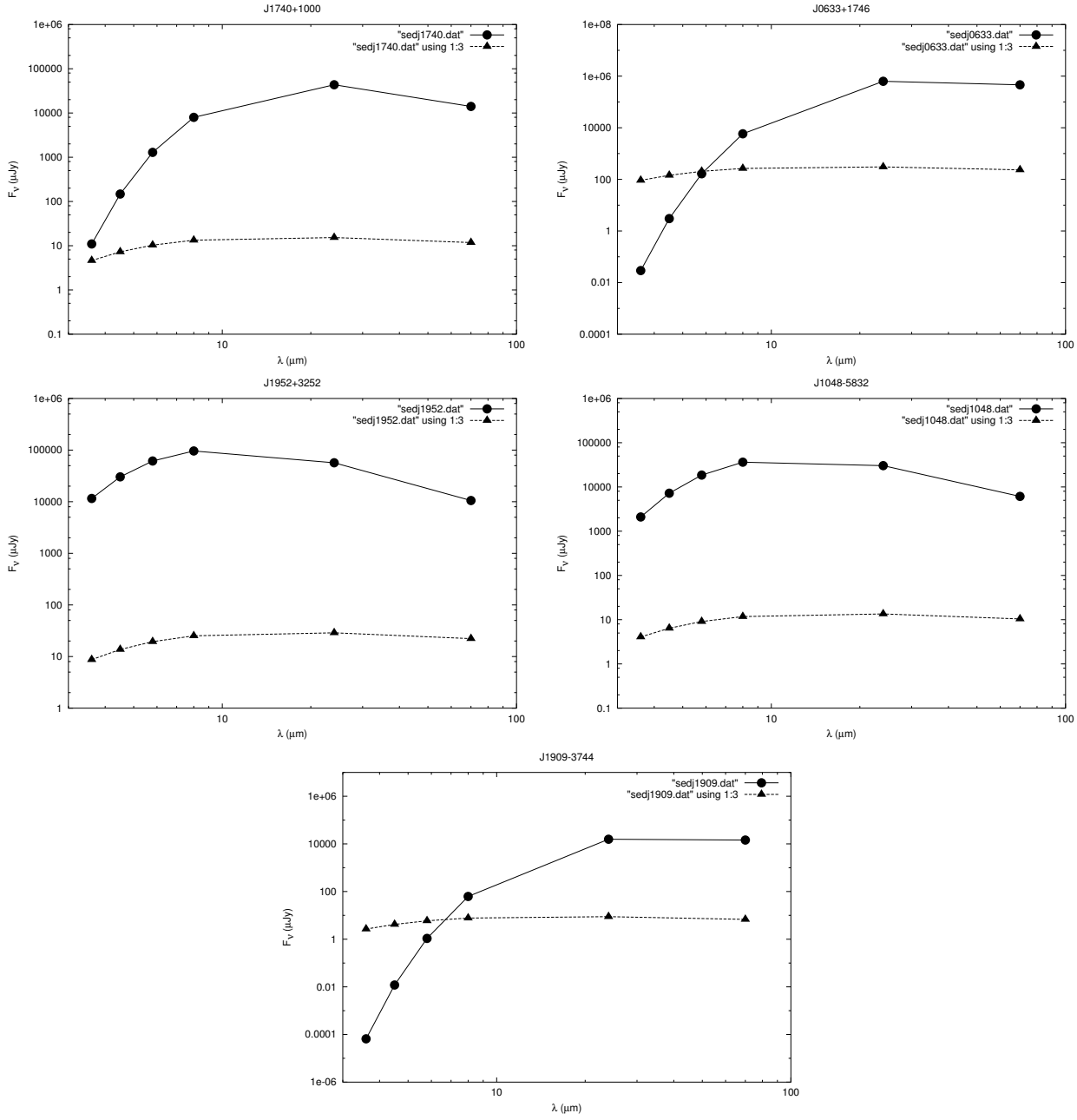

Fig. 3.— Predicted spectral distribution for all pulsars (excluding those in Fig. 1 & 2) at IRAC and MIPS wavelengths The circles and triangles denote models A and B, respectively.

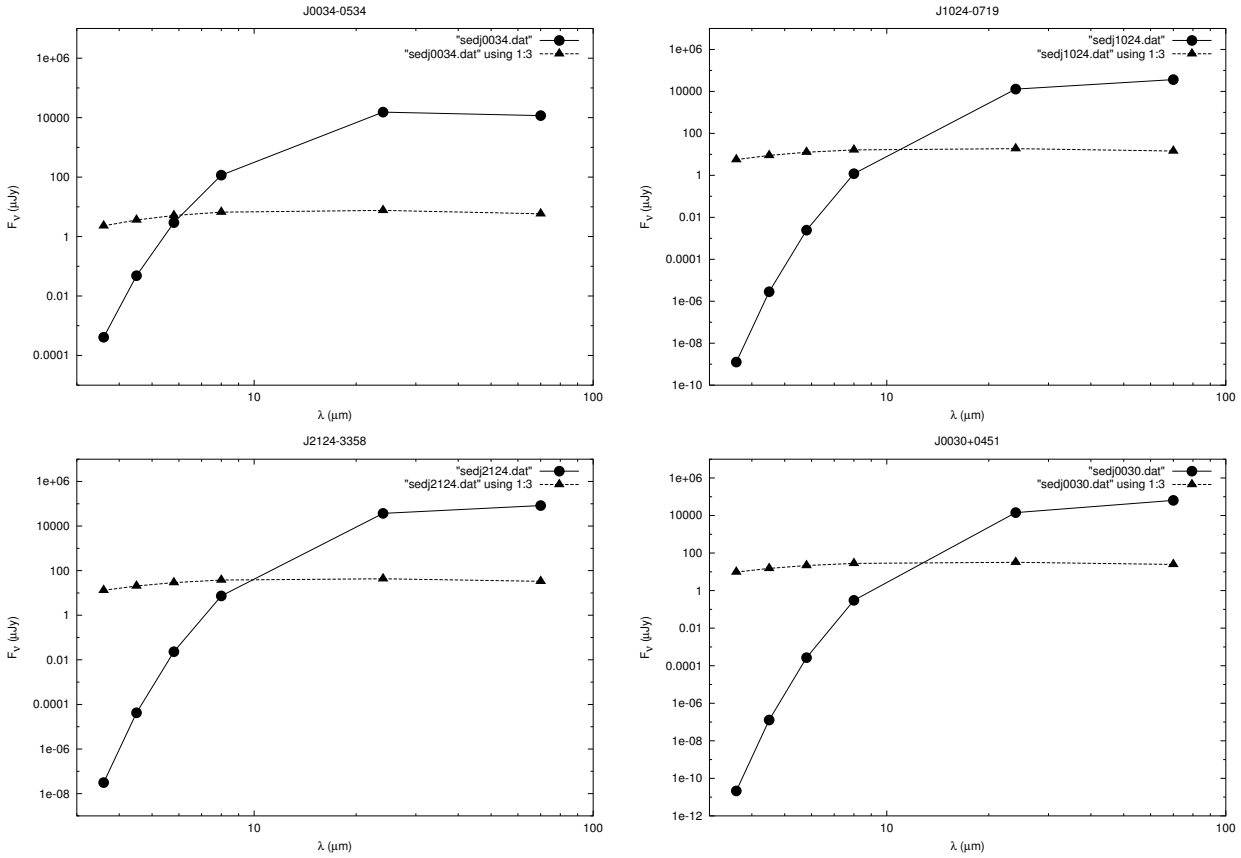

Fig. 3 (ctnd.).— Predicted spectral distribution for all pulsars (excluding those in Fig. 1 & 2) at IRAC and MIPS wavelengths The circles and triangles denote models A and B, respectively.

Table 1. Target Pulsar Sources

Name	d (kpc)	P (ms)	$\dot{P}$	L_{SD} (erg/s)
J0437-4715	0.14	5.76	5.7×10^{-20}	1.2×10^{34}
J2229+6114	12.03	51.62	7.8×10^{-14}	2.2×10^{37}
J1740+1000	1.36	154.09	2.1×10^{-14}	2.3×10^{35}
J0633+1746	0.16	237.09	1.1×10^{-14}	3.3×10^{34}
J1952+3252	2.50	39.53	5.8×10^{-15}	3.7×10^{36}
J1048-5832	2.98	123.67	9.6×10^{-14}	2.0×10^{36}
J1909-3744	0.82	2.95	1.4×10^{-20}	2.2×10^{34}
J0034-0534	0.98	1.88	5.0×10^{-21}	3.0×10^{34}
J1024-0719	0.35	5.16	1.8×10^{-20}	5.3×10^{33}
J2124-3358	0.25	4.93	2.1×10^{-20}	6.8×10^{33}
J0030+0451	0.23	4.87	1.0×10^{-20}	3.4×10^{33}

Table 2. IRAC Observing Times

Pulsar	Total time (s)
J0437-4715*	1348
J2229+6114	531
J1740+1000	1347
J0633+1746*	974

Note. — * Denotes observations which assume predicted flux values from Model B; all others use Model A.

Table 3. MIPS Observing Times

Pulsar	Total time (s)	Bands Observed
J0437-4715*	749	24μm only
J0034-0534	1208	Both
J1952+3252	1340	Both
J1048-5832	297	24μm only
J2229+6114	297	24μm only
J1909-3744	944	Both
J1740+1000	944	Both
J0633+1746*	749	24μm only
J1024-0719	548	Both
J2124-3358	548	Both
J0030+0451	548	Both

Note. — * Denotes observations which assume predicted flux values from Model B; all others use Model A.